

## Effect of Humidity on Fracture Mechanism of Age-hardened Al Alloys under Ultrasonic Loading

**Norio Kawagoishi<sup>1,\*</sup>, Kohji Kariya<sup>1</sup>, Hironori Matsusako<sup>2</sup>  
Yuzo Nakamura<sup>3</sup>, Xishu Wang<sup>4</sup>, Qingyuan Wang<sup>5</sup>**

<sup>1</sup> Department of Mechanical System Engineering, Daiichi Institute of Technology, Kirishima 899-4395, Japan

<sup>2</sup> All Nippon Airways Co., Tokyo 105-7133, Japan

<sup>3</sup> Department of Mechanical Engineering, Kagoshima University, Kagoshima 890-0065, Japan

<sup>4</sup> Department of Engineering Mechanics, Tsinghua University, Beijing 100084, China

<sup>5</sup> Department of Civil Engineering & Mechanics, Sichuan University, Chengdu 610065, China

\* Corresponding author: n-kawagoishi@daiichi-koudai.ac.jp

**Abstract** Effect of humidity on the propagation mechanism of a fatigue crack in age-hardened Al alloy 2017-T4 was investigated under ultrasonic loading in relative humidity of 25% and 85%, respectively. Plain specimen of both extruded and drawn Al alloys were tested. In the extruded alloy, fatigue cracks that propagated macroscopically in tensile mode in low humidity changed to extend in shear mode to failure, comparing to that fatigue cracks always grew in shear mode in high humidity. On the other hand, in the drawn alloy, fatigue cracks propagated in tensile mode to final fracture in low humidity, and in a combined mode of tensile and shear in high humidity. In the both alloys, the growth of cracks shorter than a specific length, e.g. ~1 mm, which is stress level dependent, was accelerated in high humidity, but it was not or little influenced by humidity beyond that specific length. The difference in fatigue crack propagation behavior between the two alloys and the effect of humidity on the fracture mechanism were discussed based on fractographic and crystallographic analyses.

**Keywords** Fatigue, Ultrasonic loading, Age-hardened Al alloy, Humidity, Texture

### 1. Introduction

High strength Al alloys have excellent properties such as high specific strength, corrosion resistance and easiness to recycle, from viewpoint of reduction of environment load. However, Al alloys have no definite fatigue limit, meaning that once a crack initiates it will continue to grow and lead to failure. Therefore, the fatigue property of Al alloys in long life region is important, though the examination of fatigue behavior in long life region is a time consuming task. Recently, ultrasonic fatigue test has attracted much attention because it is a time-saving technology for the evaluation of fatigue properties in long life region in comparison with the conventional low frequency fatigue method [1]. However, the effect of high frequency on fatigue properties has not been fully understood. Especially, the effect of environment such as corrosion is one of important factors to be clarified, because corrosion is a time-dependent damage and high strength metals are highly sensitive to corrosive environment [2-4].

In the present study, fatigue tests at ultrasonic frequency (20kHz) were carried out in relative humidity of 25% and 85% respectively, for two kinds of age-hardened Al alloys 2017-T4 (Al-Cu-Mg alloy), i.e. the extruded and the drawn alloys, which have nearly the same static strengths but different microstructure to investigate the effects of microstructure and atmospheric moisture on fatigue crack propagation behavior under ultrasonic loading.

### 2. Material and Experimental Procedure

Materials used were an extruded and a drawn bar of age-hardened Al alloy 2017-T4. The chemical

composition (mass %) of each alloy is shown in Table 1. The mean grain sizes of the extruded and the drawn alloys were about 13  $\mu\text{m}$  and 18  $\mu\text{m}$ , respectively. Their mechanical properties are shown in Table 2.

Figure 1 shows inverse pole figure on the cross section of the bars. The extruded alloy has marked texture on (111) plane, but a specified orientation is not observed in the drawn one. This difference in texture may be related to the difference in severity during fabrication processes. From the material properties of both alloys mentioned above, the important difference in both alloys is the degree of texture.

Table 1. Chemical composition (mass %)

	Si	Fe	Cu	Mn	Mg	Cr	Zn	Ti
Extruded	0.42	0.3	4.06	0.73	0.58	0.05	0.02	0.05
Drawn	0.41	0.32	3.87	0.7	0.62	0.04	0.03	0.04

Table 2. Mechanical properties

	$\sigma_{0.2}$ (MPa)	$\sigma_B$ (MPa)	$\sigma_T$ (MPa)	$\phi$ (%)
Extruded	350	471	638	32.4
Drawn	303	464	718	43.7

$\sigma_{0.2}$ : 0.2% proof stress     $\sigma_B$ : Tensile strength  
 $\sigma_T$ : True breaking stress     $\phi$ : Reduction of area

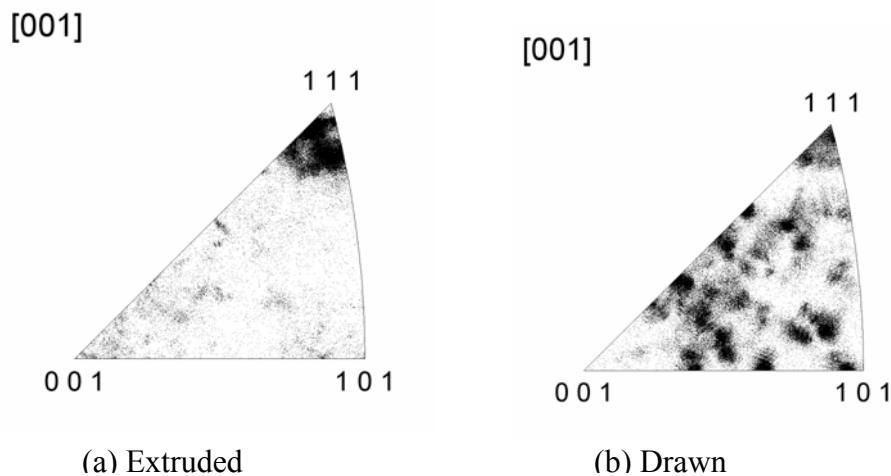


Figure 1. Inverse pole figure

Figure 2 shows shape and dimensions of specimens. Prior to fatigue testing, all of the specimens were slightly electro-polished by 40  $\mu\text{m}$  in diameter to remove the work affected layer and secure direct surface observation. The observation of fatigue damage and the measurement of crack length were conducted under a scanning electron microscope (SEM) or under an optical microscope by using the plastic-replica technique. Surface crack length,  $\ell$ , was measured in the circumferential direction of the specimen in both tensile and shear mode propagations. The crystallographic analysis was performed by using Electron Back Scatter Diffraction Pattern (EBSD) method. The fatigue tests were carried out using a 20 kHz piezoelectricity actuated ultrasonic machine in relative

humidity (RH) of 25% and 85%. In addition, rotating bending fatigue tests (50Hz) were carried out in nitrogen gas ( $N_2 > 99.995\%$ ,  $O_2 < 5\text{ppm}$ ,  $H_2O < 10\text{ppm}$ ) and RH25% to investigate the effects of oxygen and humidity. In the ultrasonic fatigue, pulse-pause tests were employed with a pulse length of 1s and a pause length of 5s to reduce temperature rise under high frequency cycling. By this method, temperature rise during ultrasonic fatigue was controlled below 3K. The humidity conditions were selected by considering the daily humidity and the significant influence of humidity on fatigue strength [4]. The deviation of humidity was controlled in the range of  $RH \pm 5\%$  with the temperature at  $298 \pm 3\text{K}$  in each humidity condition.

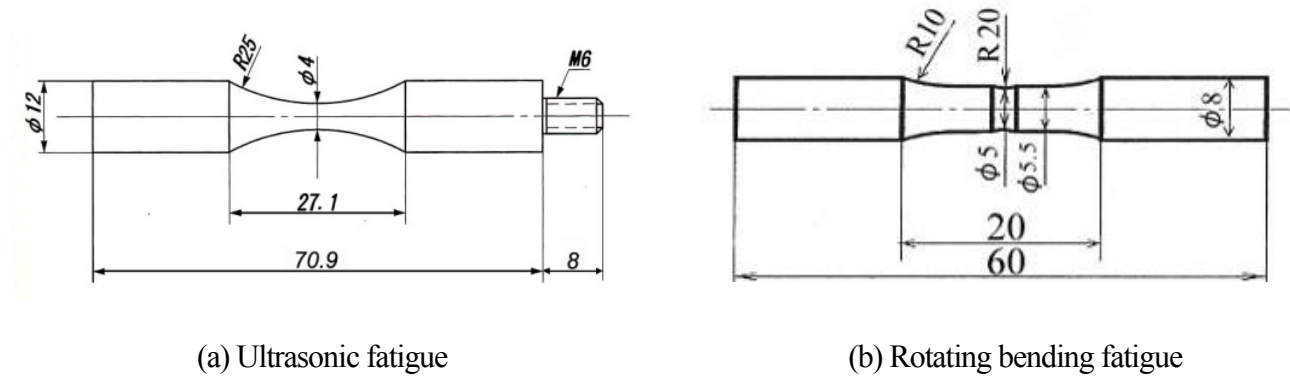


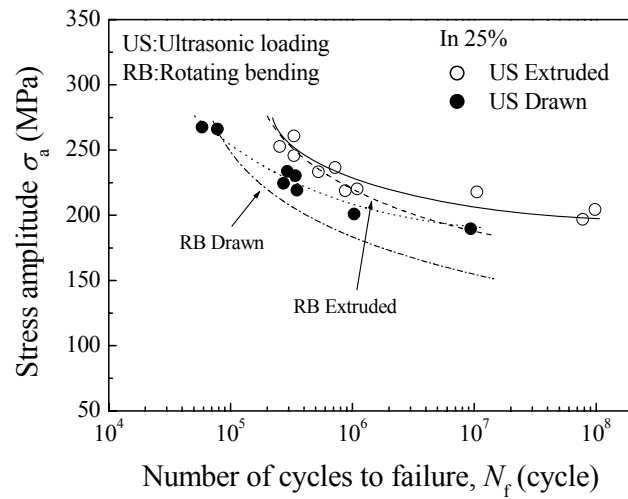
Figure 2. Shape and dimensions of specimens (mm)

### 3 Experimental Results and Discussion

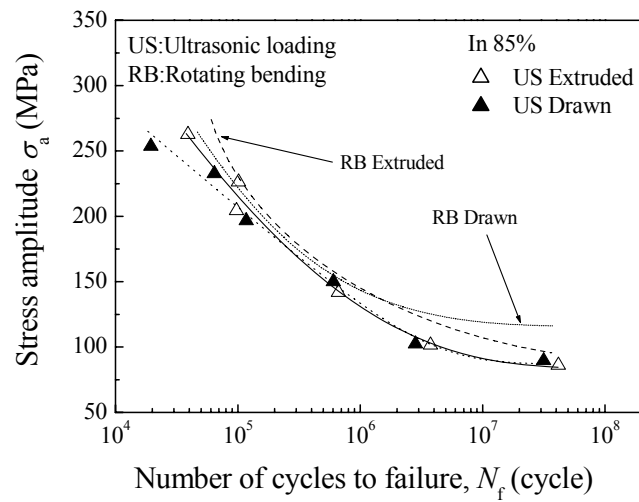
Figure 3 shows  $S-N$  curves of both alloys in RH25% and RH85%. In Fig. 3, results under rotating bending fatigue tests were also displayed by lines only [5]. Fatigue strength is larger in ultrasonic loading than in rotating bending in both alloys. Moreover, fatigue strengths of both alloys in both fatigue tests were largely decreased in high humidity with the drop in fatigue strength is larger under ultrasonic loading than under rotating bending, though the time consumed at given fatigue life was much shorter in ultrasonic fatigue. The effect of humidity on fatigue strength was larger in the extruded alloy than in the drawn one. For example, fatigue strength at  $10^7$  cycles of the extruded alloy in RH85% was decreased to about 30% of that in RH25%.

Figure 4 shows crack propagation curves of both alloys. In both alloys, a crack initiated at the early stage of stress repetitions, so most of fatigue life was occupied by the growth life of a crack in both humidity. Moreover, the propagation of cracks shorter than a specified length  $\ell_0$ , e.g. about 1 mm, was accelerated in high humidity, and there was no or little influence of humidity on the propagation of a fatigue crack over  $\ell_0$ . The existence of crack length  $\ell_0$  is clearly confirmed in RH25%, though the value of  $\ell_0$  changed with stress level.

Optical feature of surface cracks and SEM morphology of fracture at different stage of crack growth are shown in Fig. 5, in which the results of Fig. 4 are rearranged into two groups so as to better understand whether or not and how the humidity affects crack growth behavior in the two alloys. It is found that the crack growth in each alloy can be classified into two regions, i.e. region I and II. In the region I ( $\ell < \ell_0$ ), crack growth is accelerated by high humidity, while in the region II ( $\ell > \ell_0$ ), no distinct effect of humidity is recognized. In the extruded Al alloy, cracks propagated in tensile mode



(a) In RH25%



(b) In RH85%

Figure 3. *S-N* curves of extruded and drawn Al alloys

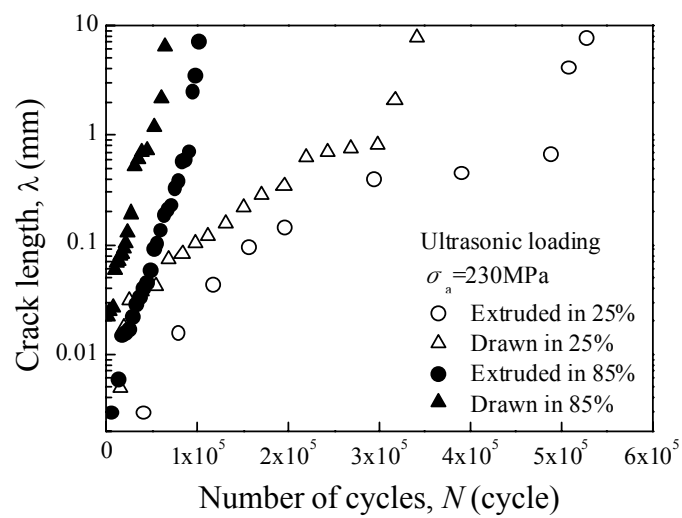


Figure 4. Crack growth curves of extruded and drawn Al alloys

macroscopically, then changed growth mode to shear one in low humidity (D), in comparison with that the whole fatigue crack propagation process was occupied by shear mode cracks in high humidity (C). The crack length corresponding to the above mentioned crack growth mode change coincides with the specific length,  $\ell_0$ , as described before. The angle between the propagation direction of the shear mode crack and the load axis,  $\theta$ , is about  $35^\circ$ . In the drawn Al alloy, however, fatigue cracks propagated in tensile mode entirely in low humidity (J) and in a combined mode of tensile and shear in high humidity (I). On the other hand, fracture morphology also depends on the microstructure of the alloy and humidity. In the extruded alloy, fracture surfaces are different even in the same propagation of a macroscopic shear mode crack. For example, fracture surfaces in the region II in RH25% (E) and RH85% (A) are mostly occupied by slip planes, while those in the region I in RH85% (B) feature with ripple-like pattern in addition to slip planes. On the other hand, in case of the drawn alloy which is characteristic of a macroscopic tensile mode crack in both humidity, many facets of a grain size and tearing of matrix between facets are observed in the regions I and II in RH25% (K, L), and in the region II in RH85% (G), though ripple-like pattern is also observed in the region I in RH85% (H). These facets are confirmed as slip planes by etch pit method (Fig. 6) and by EBSD analysis. Moreover, there was no brittle facet observed as in the corrosion fatigue of Al alloys [6] and high strength steels [7].

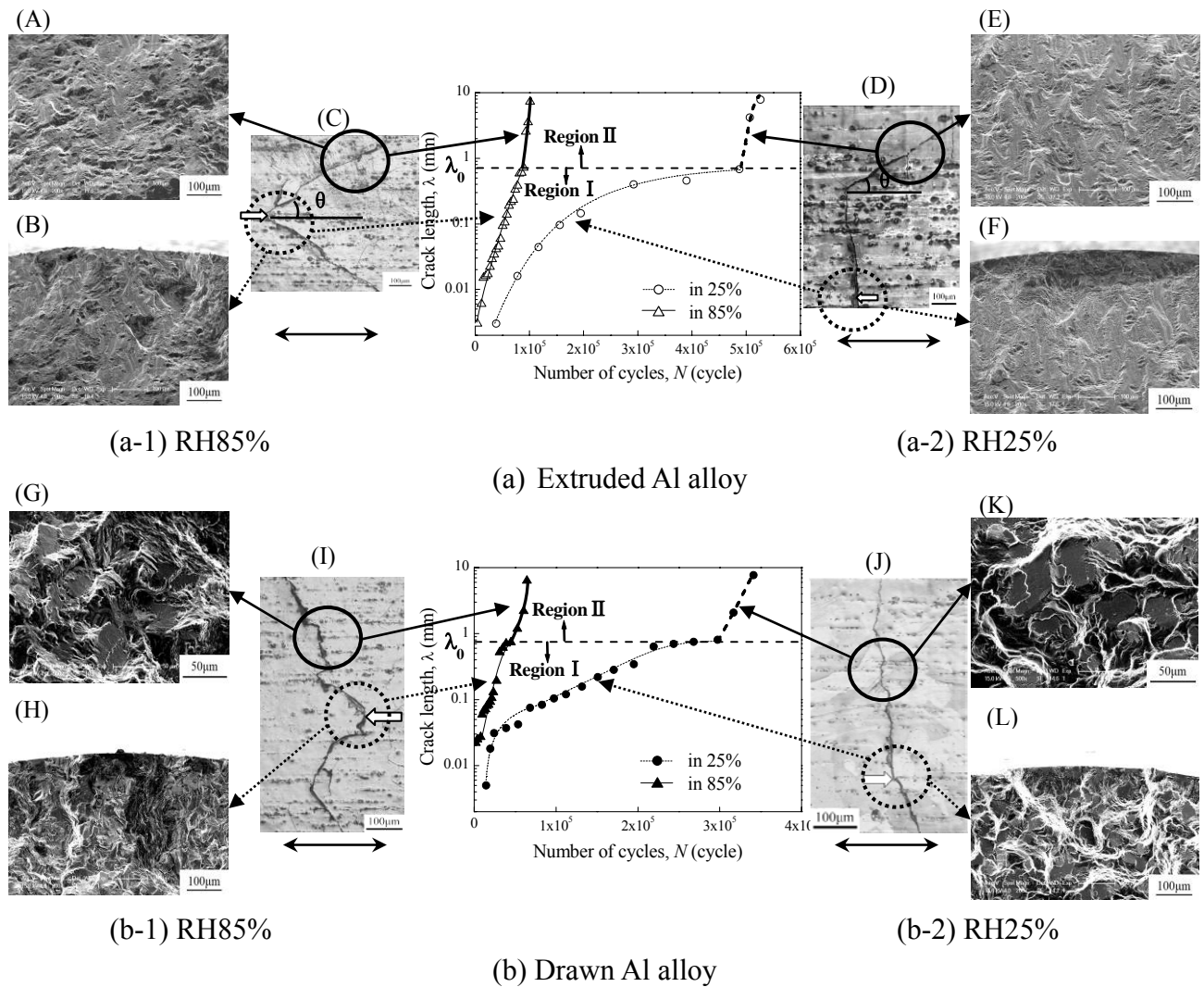


Figure 5. Optical photos featuring surface cracks and SEM micrographs characterizing fracture morphology at different stage of crack growth ( $\longleftrightarrow$  : axial direction,  $\Rightarrow$  : crack initiation site )

The observation of fracture surfaces caused by the propagation of a macroscopic tensile mode crack in low humidity, e.g. (F) and (L), was difficult because of the severe contacting at crack tips. However, striations were recognized on the fracture surface of extruded Al alloy 7075-T6 under ultrasonic loading [8], which means that cracks propagated in a ductile manner regardless of humidity. As stated above, fracture mechanism is different depending on humidity when the crack length is smaller than  $\ell_0$ , but there is no difference in fracture mechanism when the crack length is larger than  $\ell_0$  in both alloys. These findings on the effect of humidity on fracture mechanism agree well with those on crack propagation rate as shown in Fig. 4.

From the results mentioned above, it is concluded that the shear mode crack propagated along slip planes, therefore, cracks in the extruded alloy propagated in shear mode macroscopically because of

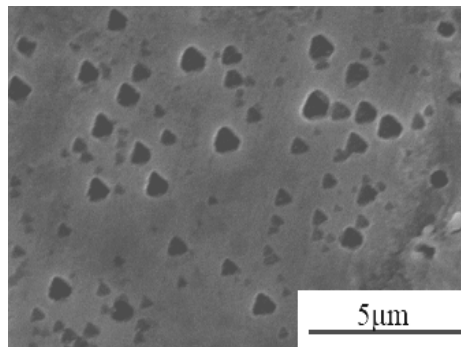
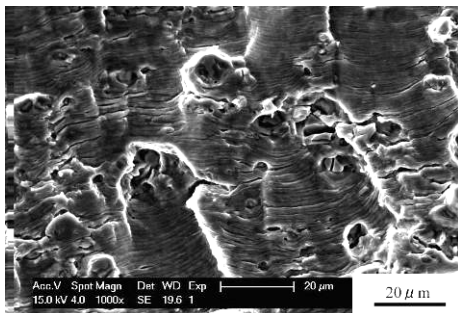
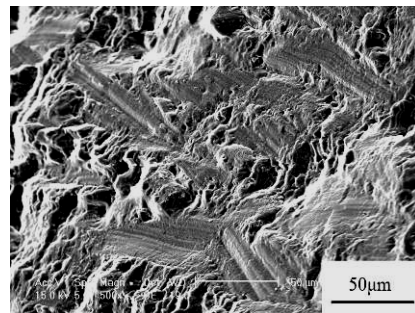


Figure 6. Etch pit figure observed at fracture surface in drawn Al alloy

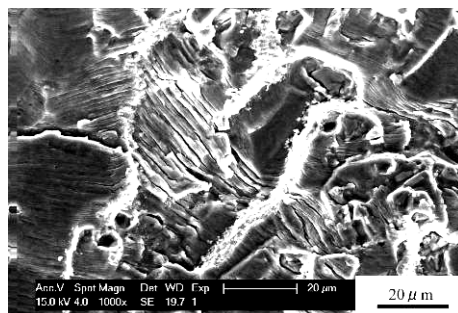


(a-1) RH25%

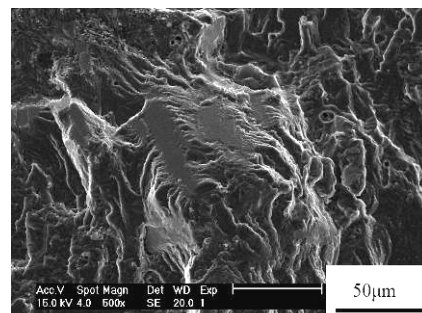


(a-2) N<sub>2</sub> gas

(a) Extruded alloy



(b-1) RH25%



(b-2) N<sub>2</sub> gas

(b) Drawn alloy

Figure 7. Fracture surfaces under rotating bending

its marked texture. This can be explained by considering that the angle between the propagation direction of the shear mode crack and the load axis,  $35^\circ$ , is related to the angle between the composed plane (100) of fracture surface with the plane (111) of texture. On the other hand, the effect of humidity on crack propagation behavior may be explained as follows. A crack whose growth was accelerated in high humidity propagated in a ductile manner, which means that fatigue deformation was assisted by hydrogen because the hydrogen enhanced localized plasticity (HELP) [9] is assumed as the propagation mechanism of a fatigue crack in high humidity. Moreover, the reason for the indistinct effect of humidity on crack propagation behavior in the region II may be related to the high crack growth rate under ultrasonic loading or in other words, atmosphere is difficult to reach at crack tips so that the environment at the crack tips is similar to vacuum. As a result, crack propagation mode changed and the effect of humidity disappeared.

In order to confirm this assumption, fatigue tests under conventional loading frequency (50Hz) were carried out in RH25% and in nitrogen gas as well to simulate vacuum condition. Figure 7 shows fracture surfaces in the region II in both RH25% and  $N_2$  gas after rotating bending fatigue. In both alloys, fracture surfaces of specimens subjected to rotating bending in  $N_2$  gas are similar to those under ultrasonic loading, though definite striations characteristic of general propagation mechanism are observed in RH25%.

#### 4. Conclusions

Fatigue tests under ultrasonic loading frequency (20kHz) were carried out for two kinds of age-hardened Al alloys, extruded and drawn alloys of 2017-T4 (Al-Cu-Mg alloy) with nearly the same static strengths in relative humidity of 25% and 85%, to investigate the effects of microstructure and humidity on propagation behavior of a fatigue crack under ultrasonic loading. The extruded Al alloy has a marked texture with plane (111) in the cross section, but the drawn alloy has not any specified orientation. In the both alloys, the propagation of small cracks shorter than a specific length, e.g. about 1 mm, which is stress level dependent, was accelerated in high humidity, causing large decrease in fatigue strength, though there was no or little influence of humidity on the propagation of a fatigue crack beyond that length. In the extruded Al alloy, fatigue cracks propagated in tensile mode macroscopically, and then changed to grow in shear mode in low humidity, in comparison with that all of fatigue crack propagation process was occupied by the shear mode crack growth in high humidity. On the other hand, in the drawn alloy, a fatigue crack propagated in tensile mode to final fracture in low humidity and in a combined mode of tensile and shear in high humidity. Fracture surfaces caused by the propagation of a shear mode crack were covered with many slip planes. The difference in fatigue crack propagation behavior between the two alloys was mainly caused by the texture. The effect of humidity on crack propagation was yielded through the acceleration to the propagation of a ductile crack.

#### References

- [1] QY. Wang, C. Bathias, N. Kawagoishi, Q. Chen, Effect of inclusion on subsurface crack initiation and gigacycle fatigue strength, *International Journal of Fatigue*, 24 (2002) 1269–1274.
- [2] K. Komai, K. Yamaji, K. Endo, Effect of atmosphere on fatigue crack propagation of aluminum alloy,

Journal of the Society of Materials Science, Japan, 29 (1980) 162–167.

- [3] K. Endo, K. Komai, Fatigue crack growth of aluminum alloy in ultra-high vacuum, Journal of the Society of Materials Science, Japan, 26 (1977) 143–148.
- [4] N. Kawagoishi, T. Fukudome, K. Kariya, Q. Chen, M. Goto, Fatigue strength of age-hardened & extruded Al alloy under high humidity (Rotating bending and ultrasonic loading), Transactions of the Japan Society of Mechanical Engineers, Series A, 76 (2010) 1651–1658.
- [5] N. Kawagoishi, A. Higashi, Q. Chen, Y. Nakamura, K. Morino, Effect of microstructure on fatigue properties of Al alloys 2017 in high humidity, Journal of the Society of Materials Science, Japan 61 (2012) 556–563.
- [6] Haftirman, S. Hattori, T. Okada, Fatigue strength of aluminum alloys in high-humidity environment, Transactions of the Japan Society of Mechanical Engineers, Series A, 62 (1996) 1140–1145.
- [7] K. Asami, H. Emura, The influence of moisture on fatigue crack propagation characteristics of high-strength steels, Journal of the Society of Materials Science, Japan, 49 (1990) 425–431
- [8] N. Kawagoishi, M. Oki, M. Goto, Q. Chen, QY. Wang, Crack propagation behavior of Al Alloy 7075-T6 under ultrasonic fatigue, Transactions of the Japan Society of Mechanical Engineers, A, 72 (2006) 1356–1363.
- [9] P.J. Ferreira, I.M. Robertson, H.K. Birnbaum, Hydrogen effects on the interaction between dislocations, Acta Materialia, 46 (1997) 1749–1757.